Available online at www.sciencedirect.com
ScienceDirect
C. R. Chimie 12 (2009) 70–84
COMPTES RENDUS CHIMIE
http://france.elsevier.com/direct/CRAS2C/

Full paper / Mémoire

Competition, resolution, and rotational motion in frustrated liquid crystals

John W. Goodby*, Stephen J. Cowling, Verena Görtz

Department of Chemistry, University of York, York YO10 5DD, UK

Received 4 June 2008; accepted after revision 3 July 2008
Available online 17 November 2008

Abstract

In this article we highlight the packing of chiral molecules in the stabilisation of twist grain boundary phases of liquid crystals. We probe the nature and structure of the screw dislocations in these frustrated phases, and describe their mobility through examples of twist inversion, reentrancy and rotational motion. We then explore the possibility of forming edge dislocation phases through investigating the filamentary structures formed at the transition from the nematic phase in bent-core systems. ***To cite this article: J. W. Goodby et al., C. R. Chimie 12 (2009).***

Résumé

Dans cet article nous mettons en évidence l'emballage des molécules chirales dans la stabilisation des phases à joints de grains tordus des cristaux liquides. Nous étudions la nature et la structure des dislocations vis dans ces phases frustrées, et décrivons leur mobilité par des exemples d'inversion de torsion, de réentrance et de mouvement de rotation. Nous explorons alors la possibilité de former des phases de dislocation de vis en étudiant des structures filamenteuses formées à la transition des phases nématiques dans les systèmes coudés. ***Pour citer cet article : J. W. Goodby et al., C. R. Chimie 12 (2009).***

Keywords: Liquid crystals; Self-organising systems; Chirality; Frustrated phases; Superconductivity

Mots-clé: Cristaux liquides ; Systèmes d'auto-organisation ; Chiralité ; Phases frustrées ; Supraconductivité

1. Introduction

Liquid crystals are the quintessential self-organising molecular materials of the modern era. They are often thought of as advanced technological materials which are found in high content, low power, flat-panel displays – known to the whole world as LCDs. However, even for those who are relatively familiar with the subject, it is not often appreciated that the term ''liquid crystal'' represents a collection of over 50 separate, identifiable, states of matter, which, like other states of matter, pervade all classes of materials, and touch upon a vast number of different, and at the same time, multidisciplinary topics of research, and a plethora of practical applications.

* Corresponding author.
E-mail addresses: jwg500@york.ac.uk (J.W. Goodby), sc520@york.ac.uk (S.J. Cowling), vg501@york.ac.uk (V. Görtz).

1631-0748/$ - see front matter
doi:10.1016/j.crci.2008.07.004

The early molecular design of thermotropic liquid crystals characterised the shapes of the molecules as either rigid rods or discs, and for the most part, the study of small molecular systems dominated the field. The accepted theory to depict and explain the physical properties of such systems then was, and to this date still is that of the continuum theory. The continuum theory describes the liquid-crystalline state as an anisotropic elastic fluid possessing its own symmetry, viscosity, and elasticity parameters.

Today the most common approach to the molecular design of liquid crystals is to employ the technique of microphase segregation. At a molecular level this may involve the bonding together of dissimilar molecular fragments, for example hydrophilic and hydrophobic units, hydrocarbon and fluorocarbon entities, etc. By designing the molecular structures in this way, inherently the system will become frustrated, i.e. the like parts of the molecules will tend to pack together, and seek to distance themselves from the dissimilar parts. However, because of the dichotomous nature of the structure, frustrations in the molecular packing occur. Such frustrations can extend further to the way in which macroscopic structures are formed by liquid-crystalline materials. For example, rod-like molecules that are chiral tend to pack together to give helical or twisted structures, conversely rod-like molecules will have a propensity to pack in flat layers. These two packing constraints on the process of self-organisation can be mutually exclusive, with the result that the system seeks an alternative path of escape from the frustration. In smectic liquid crystals the escape can result in the stabilisation of a new type of phenomena known as the structurally frustrated Twist Grain Boundary (TGB) phases. In his famous analogy between superconductors and smectic liquid crystals de Gennes envisaged the formation of such frustrated mesophases based on either twist or bend deformations [1].

de Gennes predicted that a liquid-crystalline phase punctuated by a regular array of edge or screw dislocations could mediate the expulsion of imposed bend or twist deformations at a second order nematic to layered smectic A phase transition. This is similar to how, in type II superconductors, the Abrikosov flux phase mediates the expulsion of magnetic flux from the normal metal phase to the superconducting Meissner phase [2]. Following this analogy de Gennes defined two correlation lengths: (a) the smectic coherence length (ξ) which corresponds to the correlation length in superconductors and (b) the penetration depth of twist or bend deformations (λ_T) which is a function of the twist or bend elastic constants k_t and k_b respectively and analogous to the London penetration depth in superconductors. As with superconductors, a dislocation stabilised "Abrikosov" phase was then a possibility in liquid crystal systems for values of the Landau–Ginsburg parameter $\kappa = \lambda_T/\xi > 1/\sqrt{2}$. Thus, the smectic A free energy density can be given by:

$$F_A = F_F + a|\psi|^2 + c|(\nabla - iQ_o\eta)\psi|^2 + 1/2\left(b|\psi|^4\right) \quad (1)$$

and the following associations can be made:

$$\psi \Rightarrow \psi(\text{Cooper pair wave function}) \quad (2)$$

$$\eta \Rightarrow A(\text{vector potential}) \quad (3)$$

$$h = \eta \bullet (\nabla \times \eta)(\text{for twist}) \text{ and}$$

$$h = \eta \times (\nabla \times \eta)(\text{for bend}) \Rightarrow B(\text{magnetic induction}) \quad (4)$$

The smectic A free energy reduces to the Landau–Ginsburg superconductor free energy provided that $k_s = 0$ for splay and $k_t = k_b$ for twist and bend.

de Gennes noted that the introduction of twist deformations in liquid crystal systems could be achieved through the introduction of molecular chirality. Within his analogy, the effects of molecular chirality in self-organising systems may compete successfully with those of conventional self-organising properties and the formation of a dislocation stabilised structure becomes possible in the case where $\kappa > 1/\sqrt{2}$. For example, frustration is caused by the desire of rod-like molecules to form layered mesophase structures, as in the smectic A phase, and the competing need to form helical structures due to molecular chirality. As a consequence, the twist deformations are essentially expelled to form grain boundaries, resulting in a defect stabilised phase being formed where a regular lattice of screw dislocations punctuates the normal self-organised layered phase.

de Gennes' analogy for chiral systems was taken further by Renn and Lubensky, who predicted the structure of the frustrated phase, the Twist Grain Boundary (TGB) phase [3]. Its discovery by Goodby et al. [4] linked the physical understanding of phase transitions in liquid crystals with those of superconductors. The full extent of the relationships between liquid crystals and superconductors in the de Gennes analogy is summarised in Table 1 [5].

The first materials to exhibit a frustrated TGBA phase were the (*R*)- and (*S*)-enantiomers of 1-methylheptyl 4′-(4-*n*-tetradecyloxyphenylpropioloyloxy)biphenyl-4-carboxylate, shown in Fig. 1. These remarkable compounds were found to also exhibit ferroelectric and antiferroelectric phases, a frustrated ferrielectric,

Table 1
The de Gennes analogy between superconductors and liquid crystals

Superconductor	Liquid crystal
ψ = Cooper pair amplitude	ψ = density wave amplitude
A = vector potential	n = nematic director
$B = \nabla \times A$ = magnetic induction	$h = \eta \cdot (\nabla \times \eta)$ = twist
Normal conducting metal phase	Nematic phase
Normal metal in a magnetic field	Chiral nematic (N*) phase
Meissner phase	Smectic A phase
Meissner effect	Twist expulsion
London penetration depth λ	Twist penetration depth λt
Superconducting coherence length ξ	Smectic correlation length ξ
Vortex (magnetic flux tube)	Screw dislocation
Abrikosov flux phase	Twist grain boundary phase

and a flux phase which occurs at higher temperature than the TGB phase. Fig. 1 shows the structures of the phases that (*R*)- and (*S*)-enantiomers of 1-methylheptyl 4′-(4-*n*-tetradecyloxyphenylpropioloyloxy)-biphenyl-4-carboxylate pass through upon heating and cooling. The phase that is met first upon heating is the anticlinic antiferroelectric SmC_A phase where the tilts of the molecules alternate from one layer to the next. The next phase formed upon heating is the ferrielectric phase which might be considered as a set of frustrated clock-model or Ising structures [6] where there are discrete numbers of layers having one orientation relative to an opposing orientation. The next phase formed on heating is the synclinic, ferroelectric, smectic C* phase where the molecules are tilted in layers in one preferred direction. Further heating produces the paraelectric electroclinic smectic A* phase where the molecules are arranged with their long axes on average perpendicular to the layer planes. The TGBA phase occurs then between the smectic A* phase and the flux phase in the isotropic liquid. In this case there is an in-plane twist of the structure. However, the layers prefer to remain flat. The frustration is removed by periodic sets of screw defects arranged in grain boundaries which allow blocks of the smectic A* phase to be rotated relative to one another to give a supramolecular helical structure.

Since the theoretical predictions were made and the TGB phase was discovered, many hundreds of examples of materials have been found to exhibit TGB phases, and many new TGB structures have been

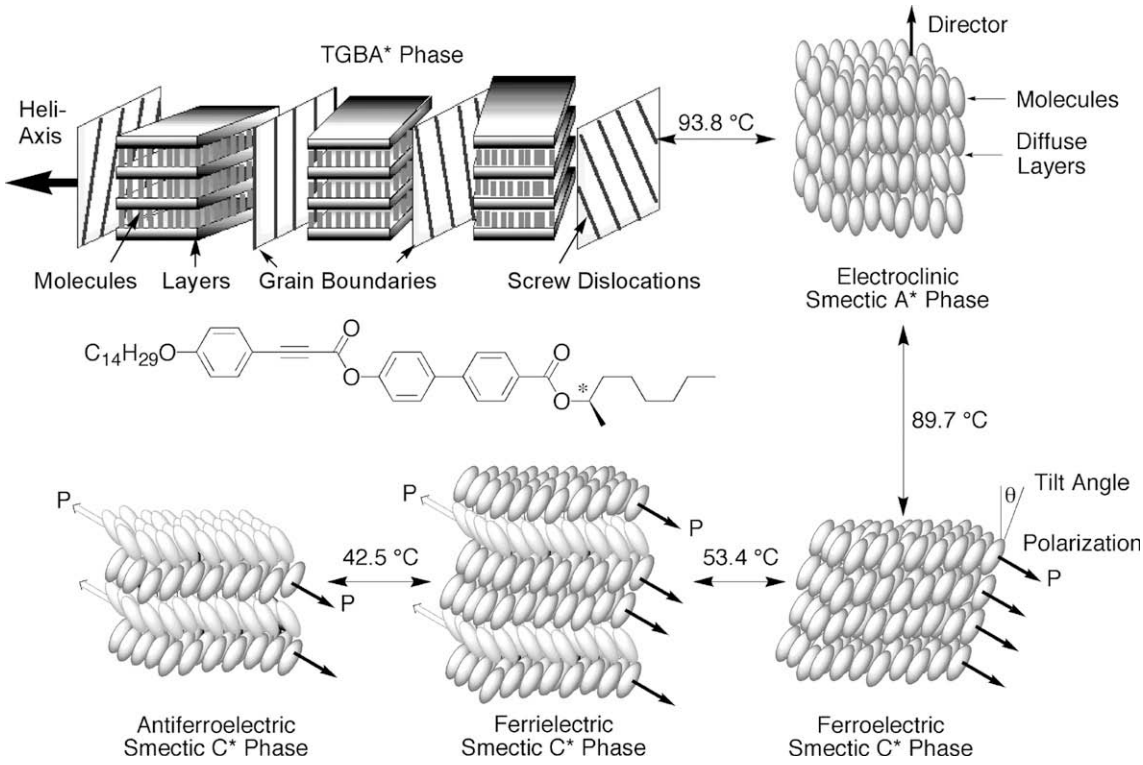

Fig. 1. (*R*)-1-Methylheptyl 4′-(4-*n*-tetradecyloxyphenylpropioloyloxy)biphenyl-4-carboxylate (14P1M7).

elucidated, e.g. Twist Grain Boundary Smectic A* phase (TGBA), Twist Grain Boundary Smectic C phase (TGBC), Undulating Twist Grain Boundary Smectic C phase (UTGBC), Giant Block Twist Grain Boundary phase (GBTGB), Anticlinic Twist Grain Boundary Smectic C_A phase ($TGBC_A$), etc. [7]. However, to our knowledge there has been no report on the equivalent Abrikosov phase stabilised by a lattice of edge dislocations in achiral materials as described in de Gennes' original theoretical model.

In this article we examine the structures of the screw dislocations in TGB phases, and their stabilities as a function of reentrancy and helix inversion. We also examine the effects that enantiomeric excess have on the stabilities of TGB phases and entangled and disentangled flux phases. Lastly, we speculate on the potential for the discovery of edge dislocation stabilised frustrated phases.

2. The structure of the screw dislocations

A screw dislocation formed in a smectic A has the structure shown in Fig. 2. The layers are cut, and on one side of the cut the layer is moved up a distance of half of the layer spacing *d*, whereas the other side is moved downwards by the same amount giving a screw dislocation having a Burgers vector, *b*, of a single layer step. Motion of the screw dislocations is in a direction parallel to the layers and perpendicular to the Burgers vector.

In the Twist Grain Boundary (TGB) A* phase, the equivalent of the London penetration depth, λ_T, can be defined as the penetration length of the twist distortion, and the equivalent of the coherence length, ξ, which is the correlation length of the smectic A* phase. Thus in a screw dislocation the core of the defect approximates to the smectic A* correlation length, obtained from X-ray diffraction, and a twist of 90° to the penetration depth. As the core of the defect is approached, see Fig. 3, the smectic A* layers give way to the formation of layers where the molecules are tilted with respect to the layer planes, i.e. a smectic C-like arrangement. As the core is further approached the molecules become more tilted with respect to the layer planes as the layers become more inclined relative to the long axis of the defect core. Near to the centre the layers give way to the formation of a nematic phase. As we move from the bulk smectic A* phase towards the core of the defect the materials pass continuously from smectic A* to smectic C* to nematic, and ultimately to a liquid.

The fact that materials such as 14P1M7 do not naturally exhibit chiral nematic phases means that transitions to this phase, if they were possible, would take place at lower temperatures than the smectic A* to isotropic liquid phase transition. Thus, if a material that exhibits a TGB phase is heated near to its clearing

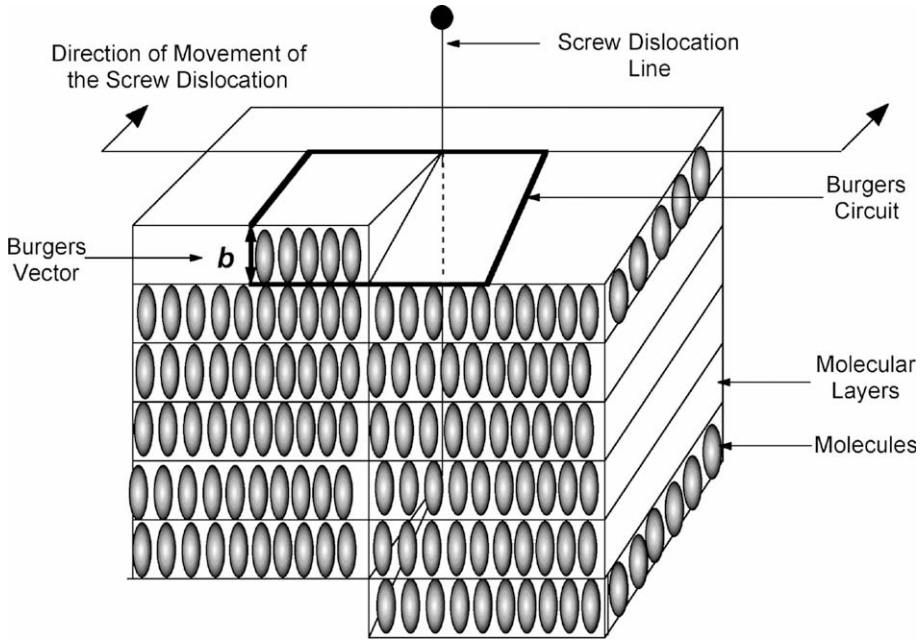

Fig. 2. Structure of the screw dislocation in a smectic A phase.

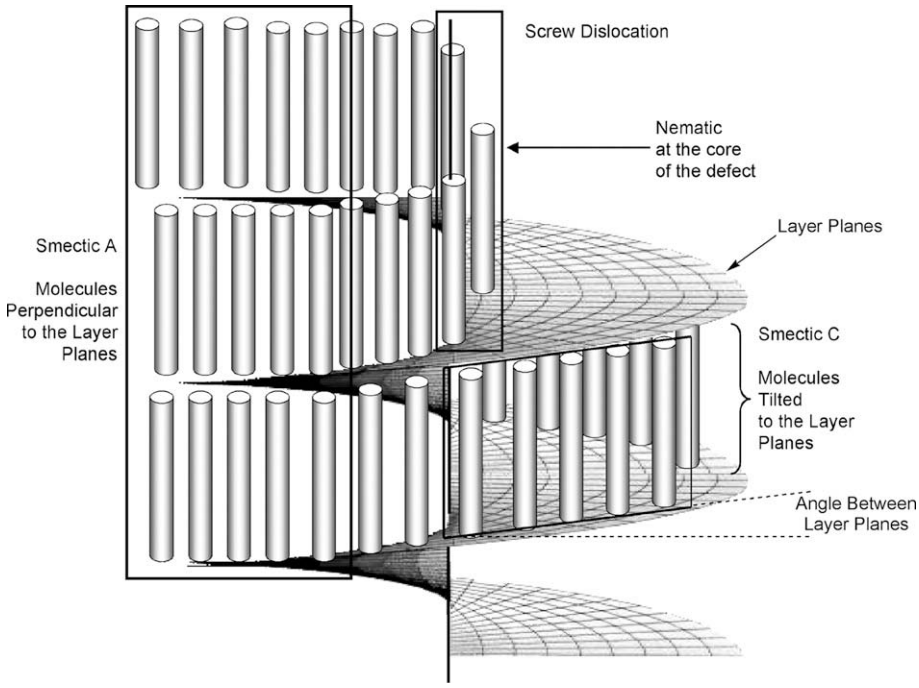

Fig. 3. Side view of a TGB screw dislocation showing the passage from smectic A* through to the chiral nematic phase at the core of the defect.

point the cores of the defects will melt first, with the cores of the defects growing. The transition to the isotropic liquid will become mediated by the formation of a disentangled flux phase, the structure of which might appear to be composed of smectic A* layers punctuated by liquid-like columns.

As we are dealing with a chiral system that forms a helical macrostructure, as shown in Fig. 1, the incorporation of screw dislocations would be expected to be periodic, with the distance between defects, l_d, being related to the twist engendered between the blocks of the normal smectic A* phase, and inversely related to the layer spacing, d. As a consequence, the screw dislocations are strung together in chains thereby forming grain boundaries, and because the phase is helical the grain boundaries are also periodic, see the schematic in Fig. 4. Furthermore, two helical forms of TGB phases are possible, one where the helical structural arrangements of the blocks or sheets between the grain boundaries are rational, i.e. the number of blocks required to form a 360° rotation of the helix is a whole number, in which case the phase is said to be ''commensurate'', see Fig. 5(a), or alternatively where the number of blocks or sheets of the normal smectic phase forming one twist of the helix is not a whole number, in which case the phase is said to be ''incommensurate'', see Fig. 5(b). X-ray diffraction quite clearly demonstrates the difference between commensurate and incommensurate TGB phases, with the latter showing a diffuse scattering whereas the former exhibits diffraction peaks where the number of spots corresponds to the relative number of grain boundaries per pitch length [7b–d,8].

Renn and Lubensky developed their models further to incorporate the chiral nematic to smectic C* transition; the phase predicted to be formed in this case was called the TGBC phase [9]. Furthermore, for the TGBC phase there are two potential structural modifications, one where the molecules in the blocks or sheets are simply inclined to the layer planes with no interlayer twist, as in an achiral smectic C phase, and another where they are allowed to form helical structures normal to the layer planes as in a normal smectic C*. These two modifications were given the preliminary designations TGBC and TGBC* respectively.

The formation of grain boundaries was confirmed by Zadazinski et al. [10]. Fig. 6 shows a high magnification view of a freeze fracture of 1-methylheptyl 4′-(4-*n*-tetradecyloxyphenylpropioloyloxy)biphenyl-4-carboxylate. The ''river'' fracture pattern, which terminates abruptly at the defect core, is characteristic of screw dislocations (see arrows in the picture). From measurements of the shadow width, it can be concluded that the screw dislocations have a Burgers

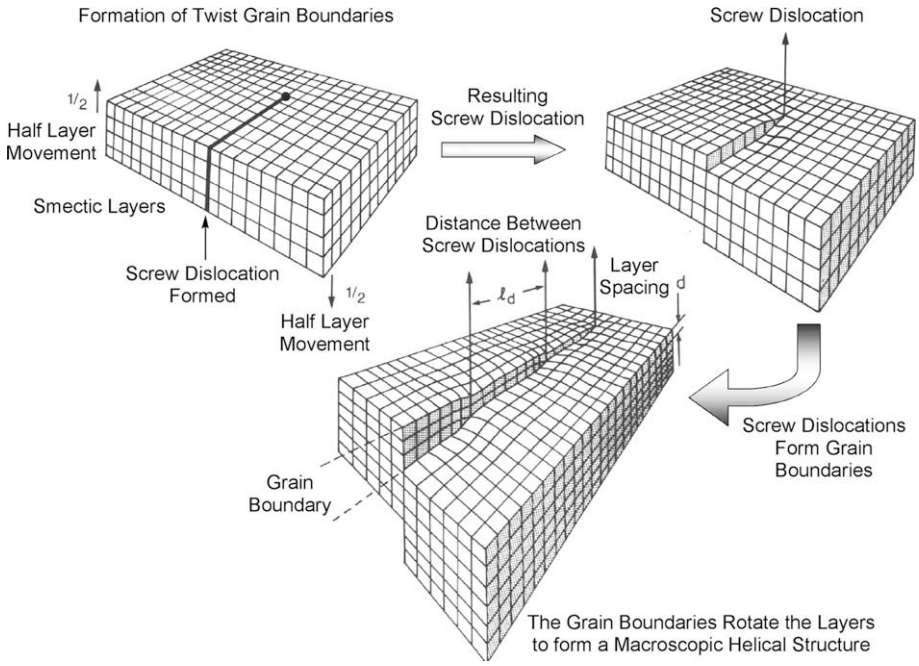

Fig. 4. A twist grain boundary in the TGB phase of liquid crystals.

vector of a single layer step, which is consistent with the model shown in Fig. 2. The screw dislocations form the twist grain boundaries that cause the orientation of the layers to change abruptly with respect to the fracture surface. The dislocations are spaced at about 15 nm apart, and the apparent layer spacing changes in discrete vertical bands from right to left as in the model of the TGBA phase. Thus the appearance of the grain boundaries in the fracture pattern is one where their separation is related to the pitch of the helical structure of the mesophase.

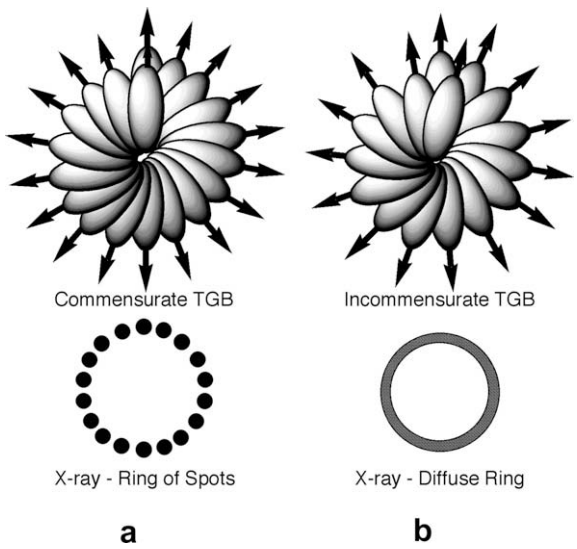

Fig. 5. Orientation along the helix axis and X-ray diffraction patterns for (a) the commensurate and (b) incommensurate TGB phases.

3. Filamentary textures

One of the most endearing and characteristic features of the TGB phase is the formation of filamentary textures, which can be observed in the transmitted polarized light microscope at low magnification (×100). Fig. 7 shows a typical filamentary texture of a TGBA phase in a free-standing film (a), and a depiction of its internal structure, with the molecular layers radiating from the axis of the filament shown below (Fig. 7(b), [11]). Indeed, because X-ray diffraction and related techniques are not able to provide data on the fine structural details of the TGBA phase, other than layer spacings, the presence of the filaments at the phase transition into the smectic A* state has been used as a diagnostic tool in the identification of TGB phases. However, it should also be noted from the analysis of the natures of the screw dislocations that the filaments will be composed of liquid-like defects, and therefore, not surprisingly the filaments tend to form curved structures, often spiralling in one preferred direction.

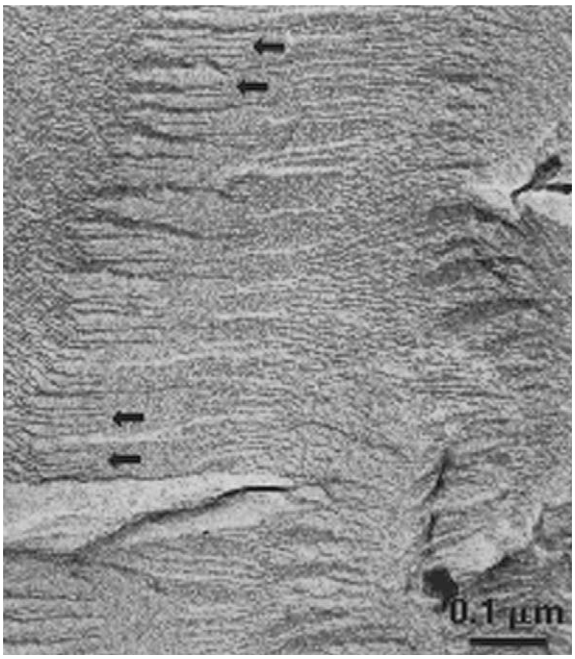

Fig. 6. A high magnification view of the fracture surface of 1-methylheptyl 4′-(4-*n*-tetradecyloxyphenylpropioloyloxy)biphenyl-4-carboxylate. Arrows highlight the screw dislocations and the smectic grains rotate discontinuously from left to right. The dislocations are spaced every 15 nm, and the shadowing shows that the dislocations have a unit Burgers vector.

4. Inversions of helical structures, reentrancy and motions of grain boundaries

The above description of the structures of TGB phases gives an impression that the grain boundaries are relatively static. However, the initial discovery of the TGB phase by Goodby indicated that the mesophase was relatively fluid [12]. Moreover, studies on various materials demonstrated that helix inversions could occur in both the TGBA and the TGBC phases [13]. In the case of the TGBA phase the inversion needs to take place through the formation of a smectic A* phase. As the inversion point is reached the helix unwinds and the separation between the grain boundaries lengthens, with some boundaries disappearing, possibly being annihilated.

For example, consider the novel esters of structure **1**, the transition temperatures for which are shown in Table 2. These materials were shown to exhibit reentrant TGBA phases where the pitch of the TGB phase changes continuously near to the transition to the smectic A* phase from either the TGB or the reentrant TGB phase.

Increasing the alkyl chain length, *R*, attached to the cyclohexane ring generally promotes the smectic A* character of the materials. However, the steric bulk of the cyclohexane ring at the terminus of the molecule disrupts the interfacial interactions between the layers in the smectic phase and allows for the chiral torque from the 1-methylheptyl group to induce the formation of TGB phases, see Fig. 8.

Interestingly, the C_3 (**1d**) and C_4 (**1e**) homologues were found to exhibit reentrant behaviour of the TGB phase. On heating, classical TGB filaments grow (see Fig. 9(a)), which then recede to give a homeotropic texture with residual birefringent halos around the air bubbles (Fig. 9(b)), and then re-grow at higher temperatures (Fig. 9(c)). This was first thought to be due to a pitch inversion occurring in the TGB phase. However, this hypothesis was rejected by examination of planar aligned textures obtained via shearing of the TGB phase. It was found that the helix was right-handed on transition from the isotropic liquid, and when the sample was cooled through the smectic A* phase a reentrant TGB phase was formed where the helix was also right-handed.

Thus the grain boundaries are very fluid, and the screw dislocations in the mesophase appear to disappear continuously rather than in a step-wise fashion as might be expected for preparations in thin cells where pinning might occur [14].

Following this study, compound **1e** (C_4 homologue) was mixed with the cyclohexane parent compound **1a** to produce a binary phase diagram as a function of temperature and concentration, see Fig. 10. The mixture studies show that as the concentration of the parent is increased (right to left in the diagram), the smectic A* phase is suppressed so that it is no longer present when the concentration of the parent compound is greater than 50%. Thus, the smectic A* phase is clearly observed as a peninsula in the phase diagram. The TGBA phase is present throughout the mixture diagram once the concentration of compound **1e** is greater than 10%.

Both compounds, **1d** (C_3) and **1e** (C_4), were carefully studied by differential scanning calorimetry, however, the transition from the TGBA–SmA* phase and from the SmA*–reTGBA phase could not be observed, with the transitions occurring without detectable enthalpies.

Across the homologous series, the enthalpy associated with the transition to the SmC* phase decreases as the alkyl chain length is increased, i.e. **1c** (0.47 kJ mol^{-1}), **1d** (0.44 kJ mol^{-1}), **1e** (0.22 kJ mol^{-1}) and **1f** (0.06 kJ mol^{-1}), whereas the enthalpies for the transitions from the isotropic liquid to TGB phases remain fairly constant: **1c** (3.9 kJ mol^{-1}), **1d** (4.2 kJ mol^{-1}),

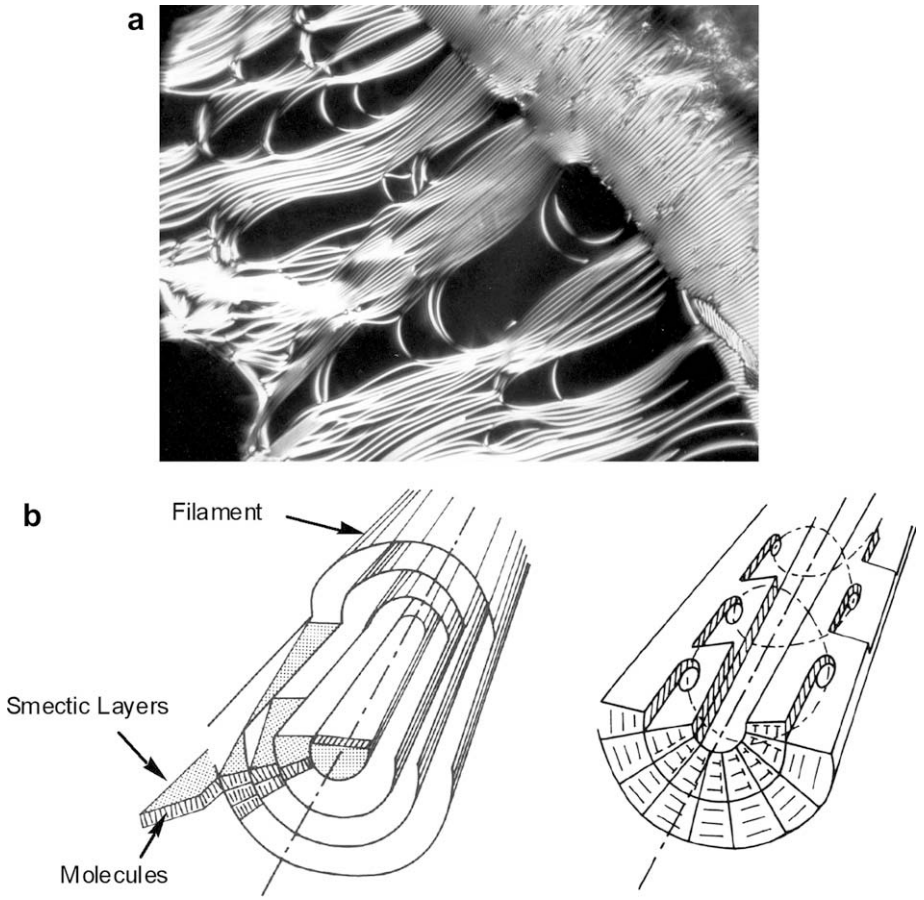

Fig. 7. (a) The filamentary texture of the TGBA phase (×100) and (b) the structure of the filaments showing the molecules as short rods in the layers of the phase.

1e (4.3 kJ mol^{-1}) and **1f** (4.7 kJ mol^{-1}). The falling value of the enthalpy values for the transition to the smectic C* phase indicates that the transition is close to being first order for the shorter homologues, whereas as the series is ascended the transition tends towards being second order. As predicted by de Gennes the TGB phases become stabilised as the transition to the more ordered state approaches second order. Reentrancy in pure materials and binary phase diagrams serves to demonstrate that the grain boundaries and hence the screw dislocations are quite mobile as the pitch of the TGB phase changes as function of temperature as the transition to the smectic A* phase approaches.

Reentrancy in the above case occurs without inversion of the helical structure, with both the normal and the reentrant phases sharing the same helical twist sense in the TGB phase. Reentrancy can also occur with inversion of the helical twist sense, and in situations where the reentrant phase has a very short temperature range, the transition from left to right could be considered as an inversion. This is the case for members of the homologous series depicted by structure **2** [15].

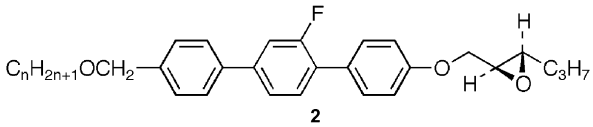

2

For this homologous series there is an inversion in the chiral nematic phase for all of the homologues, and also in the TGBC phase for the C_2 and C_3 homologues, as shown in Fig. 11. These phases are separated by a short temperature range TGBA phase. As well as the TGBC phase helix inversion, its direction of the spontaneous polarization inverts at the same point. It was postulated that the inversion phenomena were related to the distribution of conformational species as a function of temperature [16]. The continuous change in conformer distribution is thus expected to affect the

Table 2
Transition temperatures (°C) for compounds of structure **1a–f**

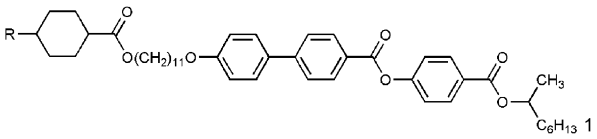

	R	Transition temperatures/°C
1a	H	K 57.7 SmC* 78.9 Iso
1b	CH_3	K 64.5 SmC* 81.8 TGBA 88.3 Iso
1c	C_2H_5	K 63.9 SmC* 77.5 TGBC 79.6 TGBA 87.9 Iso
1d	C_3H_7	K 67.8 SmC* 81.3 TGBC 83.5 TGBA 85.1 SmA* 90.8 TGBA 91.8 Iso
1e	C_4H_9	K 70.9 SmC* 77.0 TGBC 80.0 TGBA 80.9 SmA* 91.2 TGBA 92.0 Iso
1f	C_5H_{11}	K 73.1 SmC* 79.8 [TGBA + SmA*] 93.5 Iso

[TGBA + SmA*] relates to both phases coexisting at the same temperature.

structure of the screw dislocations, where the effect of one conformer species nullifies that of an opposing species, thereby increasing the pitch to infinity and reducing the polarization value to zero. The nullification could have the effect of creating liquid-like disorder along the screw axes. Moreover, the inversions occur readily and without effective pinning as the pitch changes rapidly near to the inversion point.

5. Effects of enantiomeric excess

It is quite common, as shown by the literature [17], to assume that chiral liquid crystals are 100% of one enantiomer, whereas in reality there are very, very few

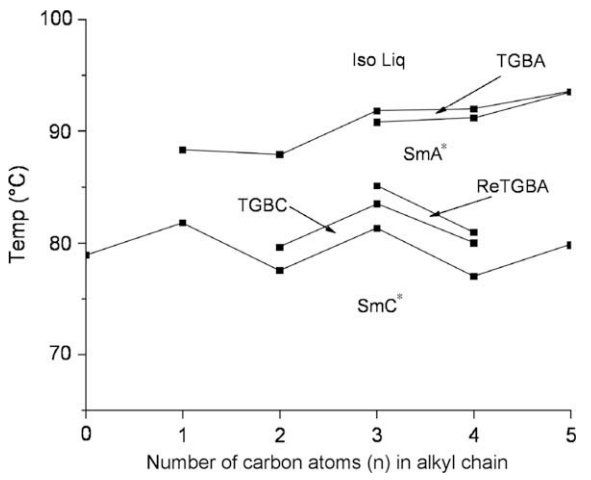

Fig. 8. Transition temperatures (°C) as a function of alkyl chain length (*n*) for compounds **1a–f**.

enantiomerically pure materials. Unlike chemical purity where the impurities can be due to a variety of substances, optical purity is dependent on the relative concentrations of both the (*R*)- and (*S*)-stereoisomers present. The less concentrated enantiomer, therefore, can act as an impurity to the other and to the self-organised system.

Optical purity, or enantiomeric excess, can affect physical properties such as the helical pitch length and the unwinding voltages for helical structures; the magnitude of the spontaneous polarization and response time in ferroelectrics; the pyroelectric and flexoelectric coefficients in non-linear systems, etc. Optical purity can directly affect the temperatures of phase transitions and mesophase stability, e.g. even at relatively high enantiomeric excesses Blue Phases, TGB phases or ferrielectric phases are not necessarily found. It is not surprising therefore that the temperature for the isotropic liquid to TGB transition is markedly affected by enantiomeric excess. For example consider the racemate and enantiomers of structure **3**, see Table 3. The racemate has an appreciably higher clearing point in comparison to either of the enantiomers (∼90% ee). The enantiomers have differing phase transition temperatures and mesophase sequences, which are both dependent on optical purity [18].

Similarly, the temperatures for the transition of the (*R*)- and (*S*)-1-methylheptyl 4′-(4-*n*-alkoxyphenylpropioloyloxy)biphenyl-4-carboxylates (14P1M7) are also affected by optical purity. Furthermore, above the clearing point transitions they exhibit enthalpies in the temperature range of the isotropic liquid. These transitions are detected as broad diffuse peaks by differential scanning calorimetry in both heating and cooling cycles. No effects are observed in the polarized microscope for this transition however, suggesting that the two liquid states have very similar properties and any ordering of the molecules in the lower temperature liquid phase must be weak. The presence of this new ‘‘quasi-liquid phase’’ was verified by X-ray diffraction and optical rotary studies [19].

It is interesting to note that when these materials are prepared in their racemic forms the liquid to liquid phase transition disappears. Moreover, the clearing temperature moves to a higher value and the magnitude of the associated enthalpy also increases, see Fig. 12 for DSC thermograms for the racemic and (*R*)-1-methylheptyl 4′-(4-*n*-tetradecyloxyphenylpropioloyloxy) biphenyl-4-carboxylates [20]. For each of the homologues that exhibit TGB phases, if the clearing point enthalpy for the liquid to TGB phase transition is

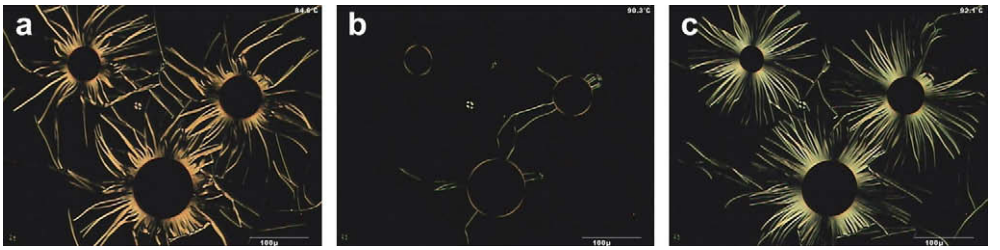

Fig. 9. Photomicrographs of **1d** taken on heating showing (a) filamentary texture of the reentrant TGBA phase, (b) homeotropic texture of the smectic A* phase, and (c) filamentary texture of the higher temperature TGBA phase (×100).

added to the value for the liquid to liquid transition, then the total value is approximately equal to that for the smectic A to isotropic transitions for the equivalent racemate.

If we consider the events occurring adjacent to, and within, the cores of the screw dislocations, as the temperature is raised it is evident that as we approach the cores of the dislocations the layers become tilted and the mesophase has the local structure of a smectic C* phase. For the 14P1M7 enantiomers, the screw axes of the dislocations are effectively composed of nematic phases, which would have lower stabilities than the surrounding smectic A* phase (if the nematic phase had a higher stability it would have been naturally exhibited by either enantiomer). Thus the core becomes liquid-like as the temperature is raised. Once the cores of the defects melt so too do the grain boundaries, and the phase forms a disentangled flux phase as opposed to an entangled flux phase. The disentangled flux phase has only short range order, however, it still appears to be optically active [21].

It is quite common for the clearing points of liquid-crystalline racemates to be higher than those of the respective enantiomers, whereas the melting points may be higher or lower depending on the material system. Thus, in order to stabilise the TGB structure the enantiomer in the least concentration might be expected to migrate towards the centres of the cores of the defects, thereby creating localised racemic modifications. By doing so the nematic phase becomes stabilised as too does the defect structure and hence the lattice of grain boundaries. This hypothesis has two consequences: (*i*) the liquid crystal phase is no longer homogeneous in terms of enantiomeric purity and (*ii*) at high optical purities the frustration is no longer stable and so the TGB phase disappears as a function of increasing enantiomeric excess. The first point is dependent on the second, and there is some limited evidence to suggest that frustrated phases are not stable at extremely high values of the enantiomeric excess.

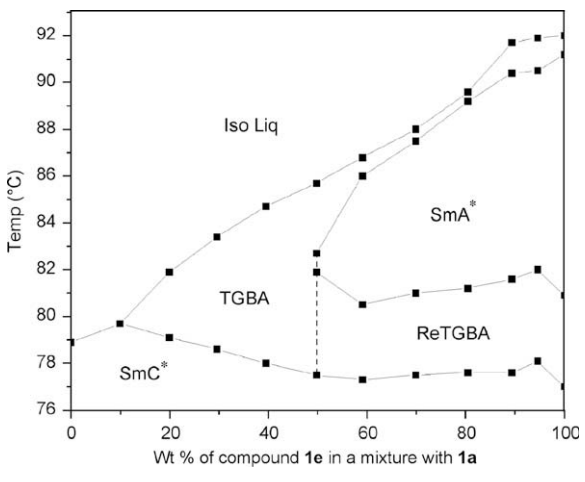

Fig. 10. Phase diagram of compound **1d** in mixtures (wt%) with compound **1a** as a function of temperature (°C).

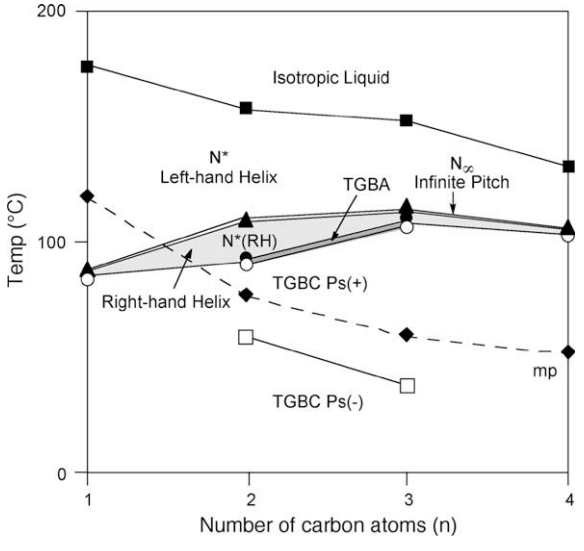

Fig. 11. Transition temperatures (°C) as a function of alkyl chain length (*n*) for homologous series **2**.

Table 3
Transition temperatures (°C) and enthalpies of transition [kJ mol^{-1}] for the racemate **3a** and (*R*)- and (*S*)-enantiomer of parent system **3** [18]

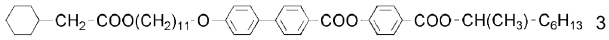

3a (*R*/*S*)	K 58.4 [54.5] SmC 77.1 [0.3] SmA 83.0 [2.1] Iso Liq
3b (*R*)	K 56.7 [50.5] SmC* 76.1 [0.6] TGBC 77.0 [-] TGBA 78.1 [1.2] Iso Liq Ps 93 nC cm^{-2} $\theta = 36°$ ee = 0.88
3c (*S*)	K 57.9 [53.4] (SmC_A* 26.2 [−]) SmC* 75.7 [0.4] TGBC 76.4 [0.8] Iso Liq Ps 98 nC cm^{-2} $\theta = 36°$ ee = 0.92

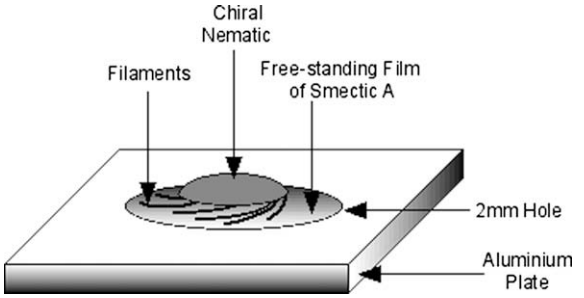

Fig. 13. Schematic of a free-standing film of a smectic A* phase that has been heated to the point where a droplet of chiral nematic phase forms on its surface. Cooling at the edges of the droplet results in the formation of filaments that spiral, and in doing so cause the droplets to rotate.

This applies to Blue phases and ferriphases as well as to TGB phases [22].

6. A TGB rotator

The mobility of the defect structure of the TGB phase can be further exemplified through the observation of rotatory motion in TGB films. For example, compound **4** [23] exhibits a chiral nematic–TGBA–SmA* phase sequence as shown. A free-standing film of the material can be drawn in the smectic A* phase. If the film is placed in a Mettler FP52 hot-stage a slight temperature gradient is obtained across the sample. Heating the material until it just starts to form a chiral nematic phase results in droplets of the chiral nematic phase appearing upon the surface of the smectic A* film. At a critical temperature the chiral nematic phase returns to the smectic A* phase via the edges of the droplets. In doing so filaments of an intermediary TGB phase can be formed, and because of the chiral nature of the material they start to curve in one preferential direction, see schematic in Fig. 13. This growth causes the chiral nematic droplet to rotate on top of the smectic A* film. Rotational rates were found to be in tens of milliseconds. Fig. 14(a) shows a droplet for a chiral nematic phase starting to spin on a free-standing film of a smectic A* phase. The filaments of the TGB phase spiral to the left, and as they grow and disappear into the smectic A* phase they cause the droplet to rotate in a clockwise direction. Fig. 14(b) shows a photomicrograph of the rotating droplet as it approaches maximum velocity. The smeared out filaments are indicative of the speed (film speed ASA400). The speed of rotation of the droplet shows that the interfacial viscosity between film and droplet is very low.

Thus the rotation is driven by a convective effect. Material from the centre of the film is converted from a smectic A* phase into an N* phase without the

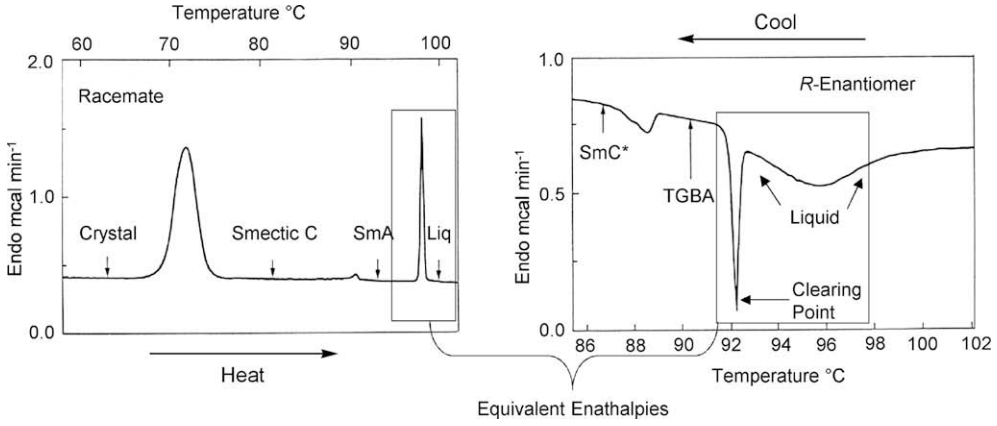

Fig. 12. Cooling thermograms taken by differential scanning calorimetry of the racemic and (*R*)-1-methylheptyl 4′-(4-*n*-tetradecyloxyphenylpropioloyloxy)biphenyl-4-carboxylates (14P1M7) [20].

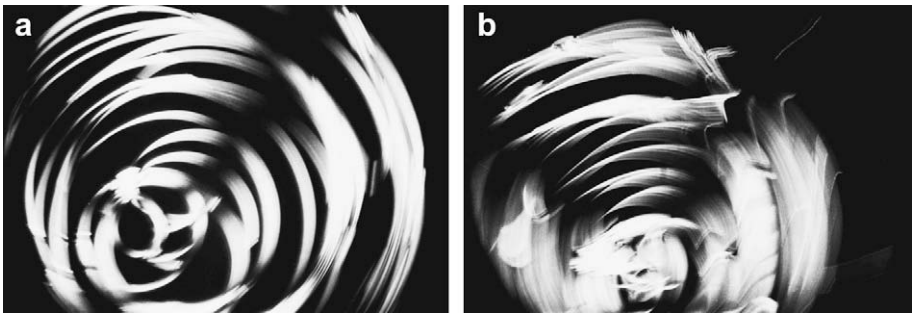

Fig. 14. (a) Filaments forming on the surface of a free-standing film of a smectic A* phase and (b) the rotation of the droplet caused by the filamentary growth (×100).

formation of a TGB phase. Cooling introduces a TGB phase via hysteresis, which converts back to a smectic A* phase, thereby completing the thermal cycle. The rotation is driven by the chirality, and so the direction of rotation will be dependent on the absolute spatial configuration of the material, thus the film provides a simple method for the determination of spatial configuration.

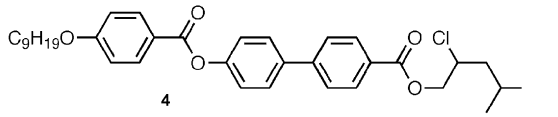

4

SmC*121.0 SmA*144.6 TGB 145.4 N* 145.5 BPI 148.6 BPII 149.9 BPIII 150.2 °C Iso Liq

7. Edge dislocation phases

In his analogy with superconductors, de Gennes postulated the formation of Abrikosov 'type II' phases in liquid crystals being stabilised by either screw or edge dislocations. The formation of screw dislocations in the TGB phase is driven through the competition between layer formation and in-plane helical twist development. Underlying the competition is the issue of molecular chirality. The local packing of the chiral molecules is at the heart of the formation of helical macrostructures, which then compete with planar layer formation. In Abrikosov phases stabilised by edge dislocations where bend deformation is the driving force for lattice formation, one might expect that such phases may be stabilised by materials that have bent molecular shapes, as shown in Fig. 15. In this case, underlying the competition is the issue of bent molecular structures. Thus, the local packing of the achiral, but bent molecules is the reason for the formation of macrostructures with intrinsic bend, which would then compete with the development of layers.

As with TGB phases, the cores of the defects of a possible bend-grain boundary (BGB) phase would be liquid-like, but approaching the defect one might expect to see the stabilisation of the core via the formation of a quasi-columnar phase.

Liquid crystals with bent molecular architectures have been the subject of intense research interest [24]. Novel ferroelectric and antiferroelectric mesophases have been discovered and characterised [25], and in many cases unusual chiral structures have been found for achiral materials. Collectively, these phases (B1–B7) are known as ''banana'' liquid crystal phases. The B7 phase has also been shown to exhibit a filamentary texture on cooling from the isotropic liquid, but unlike TGBA phases, the filaments are helical, with both left and right hand variants being present. It was postulated that the B7 phase also had a frustrated structure based

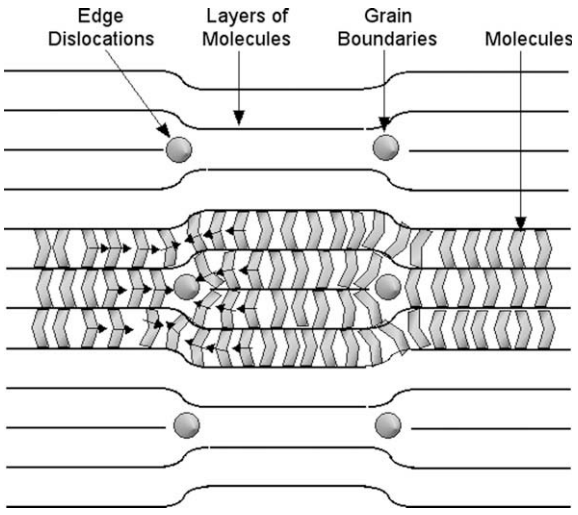

Fig. 15. Structure of an edge dislocation phase stabilised by molecules with bent gross-molecular shapes.

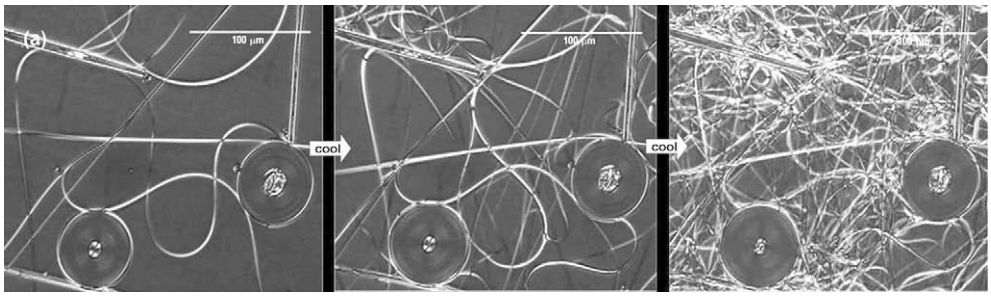

Fig. 16. Left to right: formation of filaments on cooling from 175 °C in the nematic state of compound **5** [33].

upon splay deformations associated with flexoelectric effects [26].

Interestingly, for conventional rod-like molecular systems that exhibit smectic phases Garoff noted [27] that '*since smectic phases cannot support uniform states of bend or splay, deformations caused by the flexoelectric effect must have a finite wavelength*'. For the B7 phase, where the planes of the molecules are tilted with respect to the layer planes, the layer polarity and chirality support the formation of a periodic structure of polarization splay defects, as described by Clark et al. [26]. However, if the planes of the molecules (containing the bent structure) are normal to the layer planes, as for example in the structures described as C*p* or C*B1* by Cladis et al. [28], then no opportunity for layer chirality occurs.

It has been suggested that a 'bend-grain boundary' (BGB) phase could be induced by electric fields in the nematic phase of molecules with polar structure due to their increased flexoelectric effects [29]. Indeed, Harden et al. measured a flexoelectric coefficient of $|e_3| \approx 62\ \mathrm{nC\,m^{-1}}$ for the bent-core nematic material ClP*bis*10BB, which is more than three orders of magnitude larger than that of the classic calamitic nematic material 5CB [30]. It was also suggested that some bent-core molecules may have a tendency to form a 'BGB phase' in the absence of electric fields due to spontaneous bending [29]. Hence, in the search for frustrated edge dislocation phases, it appears that the best chance of finding such a phase is in a bent-core system where the molecules have strong lateral dipoles. As with the TGB phase, an edge dislocation phase might also be expected to exhibit a filamentary defect texture. However, unlike the TGB phase the underlying phase for a bent-core system would not necessarily be smectic possessing focal-conic defects. Rather the underlying phase on cooling could be a B (banana) or columnar phase.

Consider the cooling behaviour of compound **5**. This compound exhibits a biaxial nematic phase [31], which probably needs to be considered as a splay bend modulated nematic phase with intrinsic bend [32]. It also has a large lateral dipole $\sim 4D$, and can be expected to possess strong flexoelectric properties [31].

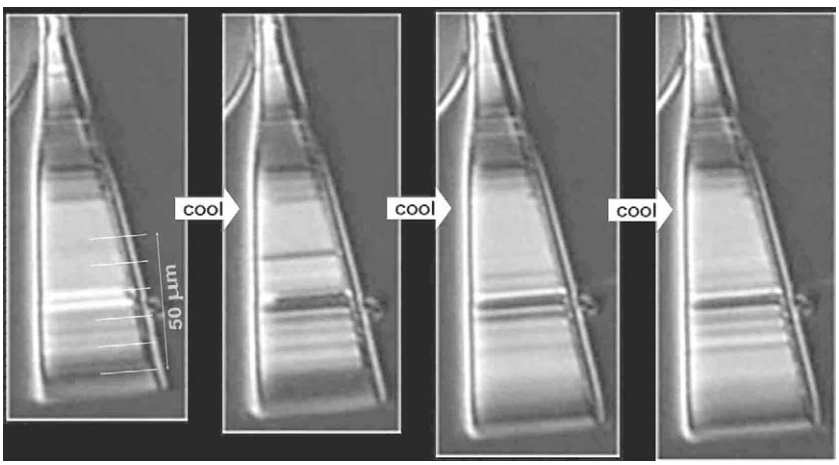

Fig. 17. Textural changes on cooling from 175 °C in a triangular area of a filament in a 5 µm cell with polyimide antiparallel planar alignment coating, crossed-polars in transmission (×100) [33].

The set of photomicrographs in Fig. 16 shows a typical sequence of events as the material was cooled [33], starting from a temperature of 175 °C, in the nematic phase. At the transition filaments were formed in a similar way to how filaments develop at a transition to a twist grain boundary (TGBA) phase for a chiral material. As the filaments grew, when they came into contact with other filaments, defect walls or air bubbles, they became curved, indicating that they are not composed of crystallites. In addition to filamentary growth, disc-like regions slowly developed on tempering. Impurity grains are seen to have rapid motions within the disc-like regions.

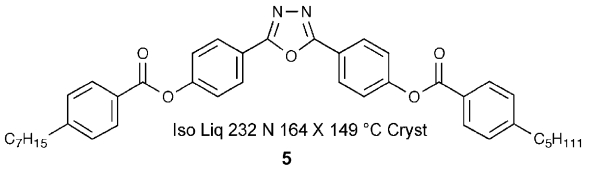

5

As the temperature was lowered, the growth and numbers of filaments increased. As more filaments were formed, the opportunities for them to bend increased, resulting eventually in the whole of the preparation becoming filled with filaments. These events took place very rapidly and over a short temperature range, which is in keeping with typical transitions to and from TGB phases.

Fig. 17 shows an expanded view of the end of a filament that had developed a triangular area. This area displays parallel lines perpendicular to the main axis of the filament that disappear and reappear and seem similar to Grandjean lines seen for chiral nematic liquid crystals. The lines are possibly dislocations or liquid-like grain boundaries, indicating that the meso-phase possesses a large scale superstructure. The spacing between the lines was approximately 6–7 μm.

Considering the presented evidence, one could speculate that indeed a dislocation lattice similar to the structure of the TGB phase for chiral materials, but based on edge dislocations, i.e. a bend-grain boundary structure, is the basis of the filamentary texture observed for this achiral bent-core compound.

8. Summary

The de Gennes analogy between superconductors and liquid crystal phases has led to the discovery of a number of novel frustrated phases, however, their physical properties have yet to be fully unfurled. Thus in this study we have investigated some fascinating and unusual properties of TGB phases, including reentrancy, twist inversion, polarization inversion, and droplet rotation. These properties demonstrate the ease with which the grain boundaries move and combine with one another. We also explored the possibility of the formation of edge dislocation phases in achiral bent-core systems with strong lateral dipoles through investigating the filamentary textures formed at the phase transition from the nematic phase in a bent-core oxadiazole system.

Acknowledgements

The authors would like to thank the Engineering and Physical Sciences Research Council (EPSRC) for financial support.

References

[1] P.-G. de Gennes, Solid State Commun. 10 (1972) 753.
[2] A.A. Abrikosov, JETP 5 (1957) 1174.
[3] S.R. Renn, T.C. Lubensky, Phys. Rev. A 38 (1988) 2132.
[4] J.W. Goodby, M.A. Waugh, S.M. Stein, E. Chin, R. Pindak, J.S. Patel, Nature 337 (1989) 449.
[5] T.C. Lubensky, Physica A 220 (1995) 99.
[6] (a) Y. Takanishi, K. Hiraoka, V.K. Agrawal, H. Takezoe, A. Fukuda, M. Matsushita, Jpn. J. Appl. Phys. 30 (1991) 2023; (b) P. Mach, R. Pindak, A.-M. Levelut, P. Barois, H.T. Nguyen, H. Baltes, M. Hird, K.J. Toyne, A.J. Seed, J.W. Goodby, C.C. Huang, L. Furenlid, Phys. Rev. E 60 (1999) 6793.
[7] (a) M. Petit, P. Barois, H.T. Nyugen, Europhys. Lett. 36 (1996) 185; (b) N. Isaert, L. Navailles, P. Barois, H.T. Nguyen, J. Phys. II (Paris) 4 (1994) 1501; (c) L. Navailles, P. Barois, H.T. Nguyen, Phys. Rev. Lett. 71 (1993) 545; (d) L. Navailles, R. Pindak, P. Barois, H.T. Nguyen, Phys. Rev. Lett. 74 (1995) 5224; (e) P.A. Pramod, R. Pratibha, N.V. Madhusudana, Curr. Sci. 73 (1997) 761; (f) J.G. Meier, P. Rudquist, A.S. Petrenko, J.W. Goodby, S.T. Lagerwall, Liq. Cryst. 29 (2002) 179.
[8] (a) A. Anakkar, A. Daoudi, J.M. Buisine, N. Isaert, T. Delattre, H.T. Nguyen, C. Destrade, J. Therm. Anal. 41 (1994) 1501; (b) Y. Galerne, Eur. Phys. J 3 (2000) 355.
[9] S.R. Renn, T.C. Lubensky, Mol. Cryst. Liq. Cryst. 209 (1991) 349.
[10] K.J. Ihn, J.A.N. Zasadzinski, R. Pindak, A.J. Slaney, J.W. Goodby, Science 258 (1992) 275.
[11] J.M. Gilli, Kamay, Liq. Cryst. 4 (1992) 545.
[12] J.W. Goodby, Struct. Bonding 95 (1999) 83.
[13] (a) H.-W. Tunger, V. Vill, J. Chem. Soc. Chem. Commun. (1995) 1047; (b) V. Vill, H.-W. Tunger, D. Peters, Liq. Cryst. 20 (1996) 547; (c) D.S. Shanker Rao, K. Prasad, V.N. Raja, C.V. Yelamaggad, S.A. Nagamani, Phys. Rev. Lett. 87 (2001) 085504.
[14] (a) M. Ismaili, F. Bougrioua, N. Isaert, C. Legrand, H.T. Nguyen, Phys. Rev. E 65 (2002) 011701; (b) M. Ismaili, F. Bougrioua, N. Isaert, C. Legrand, H.T. Nguyen, Ferroelectrics 276 (2002) 239.

[15] K. Takatoh, J.W. Goodby, R. Pindak, J.S. Patel, Proceedings of the 20th Japan Liquid Crystals Conference, Nagoya, Japan, October 1994, 1G-304, 1994. K. Takatoh, M.J. Watson, P. Styring, M. Hird, J.W. Goodby. Proceedings of the 20th Japan Liquid Crystal Conference, Nagoya, Japan, October 1994, 2G-309, 1994.
[16] (a) M.J. Watson, M.K. Horsburgh, J.W. Goodby, K. Takatoh, A.J. Slaney, J.S. Patel, P. Styring, J. Mater. Chem. 8 (1998) 1963; (b) J.S. Patel, J.W. Goodby, Philos. Mag. Lett. 55 (1987) 283.
[17] D.M. Walba, H.A. Razavi, A. Horiuchi, K.F. Eidman, B. Otterholm, R.C. Haltiwanger, N.A. Clark, D.S. Parmar, R. Shao, M.A. Wand, R.T. Vohra, Ferroelectrics 113 (1991) 21.
[18] S.J. Cowling, A.W. Hall, J.W. Goodby, Liq. Cryst. 32 (2005) 1483.
[19] J.W. Goodby, M.A. Waugh, S.M. Stein, E. Chin, R. Pindak, J.S. Patel, J. Am. Chem. Soc. 111 (1989) 8119.
[20] J.W. Goodby, I. Nishiyama, A.J. Slaney, C.J. Booth, K.J. Toyne, Liq. Cryst. 14 (1993) 37.
[21] see for example: (a) J.S. Kang, D.A. Dunmur, C.J. Booth, J.W. Goodby, K.J. Toyne, I. Nishiyama, Liq. Cryst. 19 (1995) 376; (b) C.J. Booth, J.W. Goodby, K.J. Toyne, D.A. Dunmur, J.S. Kang, Mol. Cryst. Liq. Cryst. 260 (1995) 39.
[22] P. Taborek, J.W. Goodby, P.E. Cladis, Liq. Cryst. 4 (1989) 21.
[23] (a) A.J. Slaney, Ph.D. Thesis, University of Hull, 1992; (b) A.J. Slaney, J.W. Goodby, J. Mater. Chem. 1 (1991) 5; (c) A.J. Slaney, J.W. Goodby, Liq. Cryst. 9 (1991) 849.
[24] (a) G. Pelzl, S. Diele, W. Weissflog, Adv. Mater. 11 (1999) 707; (b) R.A. Reddy, C. Tschierske, J. Mater. Chem. 15 (2005) 1 and references therein.
[25] D. Walba, Science 288 (2002) 2181.
[26] D.A. Coleman, J. Fernsler, N. Chattham, M. Nakata, Y. Takanishi, E. Korblova, D.R. Link, R.-F. Shao, W.G. Jang, J.E. Maclennan, O. Mondainn-Monval, C. Boyer, W. Weissflog, G. Pelzl, L.-C. Chien, J. Zasadzinski, J. Watanabe, D.M. Walba, H. Takezoe, N.A. Clark, Science 301 (2003) 1204.
[27] S. Garoff, Ph.D. Thesis, University of Harvard, 1977.
[28] P.E. Cladis, H.R. Brand, H. Pleiner, Ferroelectrics 243 (2000) 221.
[29] H.S. Kitzerow, Mol. Cryst. Liq. Cryst. 412 (2004) 103.
[30] J. Harden, B. Mbanga, N. Éber, K. Fodor-Csorba, S. Sprunt, J.T. Gleeson, A. Jákli, Phys. Rev. Lett. 97 (2006) 157802.
[31] (a) L.A. Madsen, T.J. Dingemans, M. Nakata, E.T. Samulski, Phys. Rev. Lett. 92 (2004) 145505; (b) B.R. Acharya, A. Primak, S. Kumar, Phys. Rev. Lett. 92 (2004) 145506; (c) C.D. Southern, P.D. Brimicombe, S.D. Siemianowski, S. Jaradat, N. Roberts, V. Görtz, J.W. Goodby, H.F. Gleeson, Europhys. Lett. 82 (2008) 56001.
[32] (a) I. Dozov, Europhys. Lett. 56 (2001) 247; (b) J. Peláez, M.R. Wilson, Phys. Rev. Lett. 97 (2006) 267801.
[33] V. Görtz, C. Southern, N.W. Roberts, H.F. Gleeson, J.W. Goodby, Soft Matter (2008). doi:10.1039/b808283a.